16. SOME TRACE ELEMENTS IN THE CARBONATE SAMPLES RECOVERED FROM HOLES 390, 390A, 391C, AND 392A OF DSDP LEG 44

Maurice Renard,[1] Réne Létolle,[1] Maurice Bourbon,[2]
and Gilbert Richebois[1]

We determined concentrations of trace elements in the carbonate fraction by atomic absorption analysis following the procedure described by Renard and Blanc (1971, 1972). The age of the samples studied range from Barremian to middle Eocene (Holes 390, 390A), Tithonian to Aptian (Hole 391C), and late Campanian to Barremian (Hole 392A). Mineralogically, they all contain low magnesian calcite. The results of the analysis are given in Tables 1 to 4.

HOLE 391C

Relationship With Insoluble Residues

In some samples, we obtained sufficient insoluble residues, following treatment with acetic acid, to relate certain element concentrations to percentage of insoluble residue (Figure 1). We noted a distinct, positive correlation between concentrations of potassium, sodium, and magnesium and the percentage of insoluble residue. (Some of these elements may have been flushed into the insoluble fraction in spite of the precautions taken.) We found a positive, but less pronounced, relationship between zinc and strontium concentrations and insoluble residue, whereas we detected no correlation between manganese concentrations and insoluble residue. Because of this relationship we consider the results obtained for potassium, sodium, and magnesium, and those obtained for strontium, and zinc, when the samples contain more than 10 per cent insoluble, to be unreliable.

Strontium

The concentration curve of strontium contents is very characteristic for samples containing more than 90 per cent carbonates (Figure 2). The amount of strontium decreases continuously from the Aptian to the Tithonian sediments; a rapid decrease occurs in the lower Valanginian-upper Barremian sediments. We attribute this to increased diagenesis with greater depth which reflects the degree of diagenesis as a function of age. This is consistent with earlier claims of Sheerman and Shirmohammadi (1969), Kinsman (1969), and Renard (1972) that strontium is a reliable measure of carbonate diagenesis. The similarity of the strontium concentrations and the sediment accumulation curves illustrates that the highest rate of sedimentation (2.8 cm/10^3 years) corresponds to the greatest loss of strontium. A rough correlation between the gradient of the strontium concentration curve and the sedimentation rate is given in Figure 3.

Manganese

We distinguished two zones in Hole 391C on the basis of the manganese concentrations (Figure 4). One zone, in lower Tithonian and lower Berriasian sediments, has high manganese concentrations. The second zone, between the upper Berriasian to the lower Aptian sediments, has low manganese concentrations. The behavior of manganese during sedimentation is complex inasmuch as it can be co-precipitated with calcium carbonate or as dioxide. In a reducing medium, co-precipitation predominates and produces low manganese carbonates; in an oxidizing medium, dioxide precipitation predominates producing "carbonates rich in manganese" (Michard, 1969). If the oxidation-reduction mechanisms alone were responsible for the variation in manganese concentrations, we would expect maximum values in the Aptian to upper Valanginian sediments, which, because they were deposited at slower rates and during a time of little subsidence, were exposed a relatively long time to an oxidizing environment. In Hole 391C, however, the greatest amounts of manganese are found in the zone characterized by a high sedimentation rate (Berriasian-Tithonian). This suggests that variations in the manganese content may reflect variations in supply of manganese to the sediment. The manganese may have had a volcanic origin, especially as volcanic glass has been found in several manganese-rich samples (391C-52-2, for example). Michard (1975) has shown that seawater in contact with basalt is strongly enriched in manganese; moreover iron- and manganese-rich hydrothermal sources were detected along certain transcurrent faults during the FAMOUS expedition of 1974 (in Michard, 1975). If we accept that the manganese in the Berriasian-Tithonian sediments has a volcanic source, then its reduction in the overlying sediments suggests a decrease of volcanic activity during late Berriasian to the end of Aptian time.

The curves giving the partition of iron and manganese concentrations show an inverse relationship (Figure 5). Manganese concentrations are always highest where iron concentrations are lowest. If the early Tithonian manganese is of volcanic origin, the iron must have a different origin, which is inconsistent with results of the FAMOUS expedition and other data, or it was precipitated as less soluble iron oxide and hydroxide near the volcanic ridge.

The Hauterivian to Barremian zone has the highest iron and the lowest manganese concentrations. Note that iron-rich samples always have a low carbonate content. The iron could then be of continental detrital origin and may reflect an early stage of the transition from a carbonate to siliciclastic depositional environment which culminated, near the end of the Upper Cretaceous, with the deposition of black

[1]U.E.R. des Sciences de la Terre, Université Pierre and Marie Curie, Paris, France.
[2]Ecole Nationale des Mines de Paris, France.

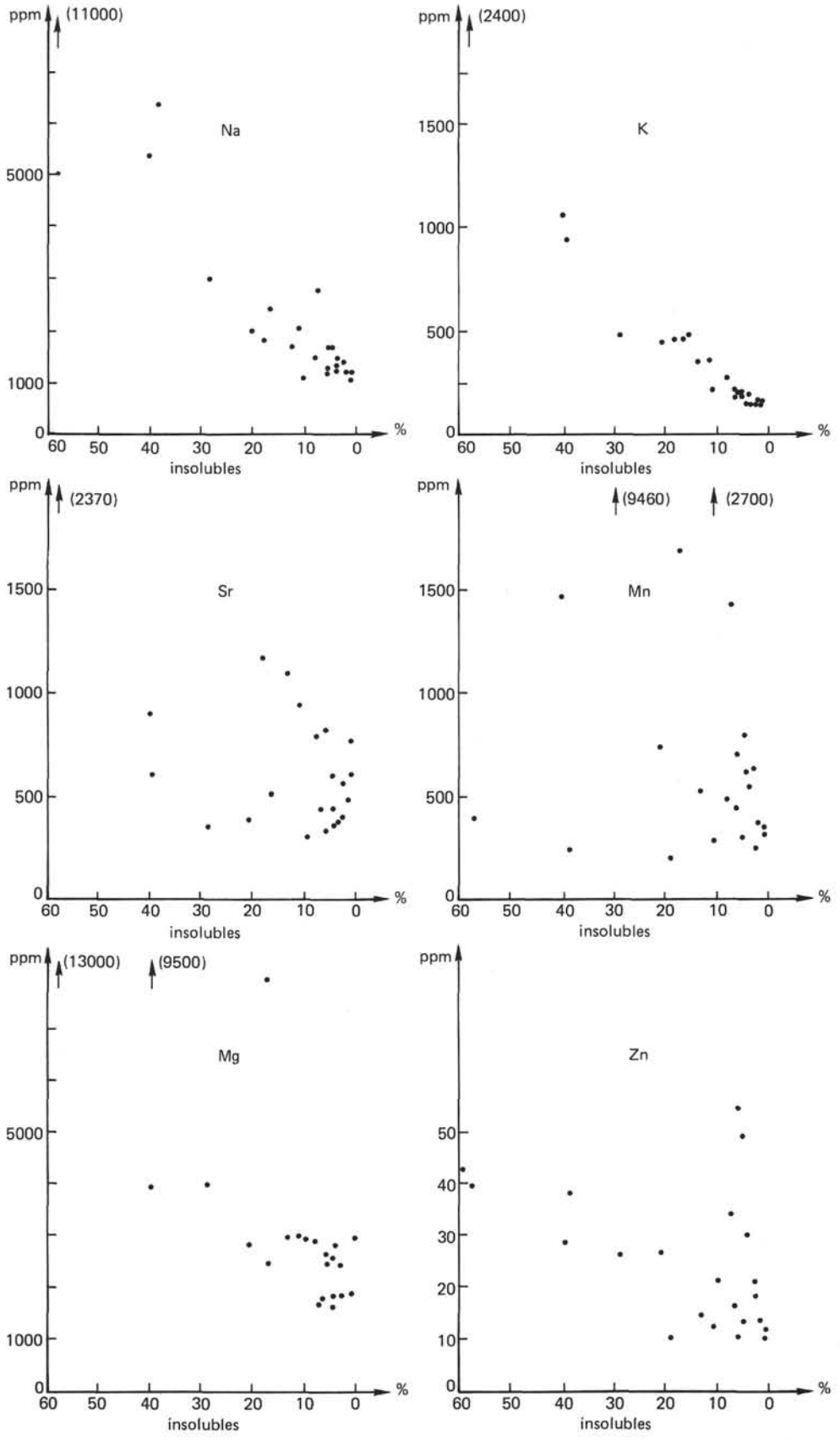

Figure 1. *Relationship between certain element concentrations and percentages of insoluble residues in Hole 391C.*

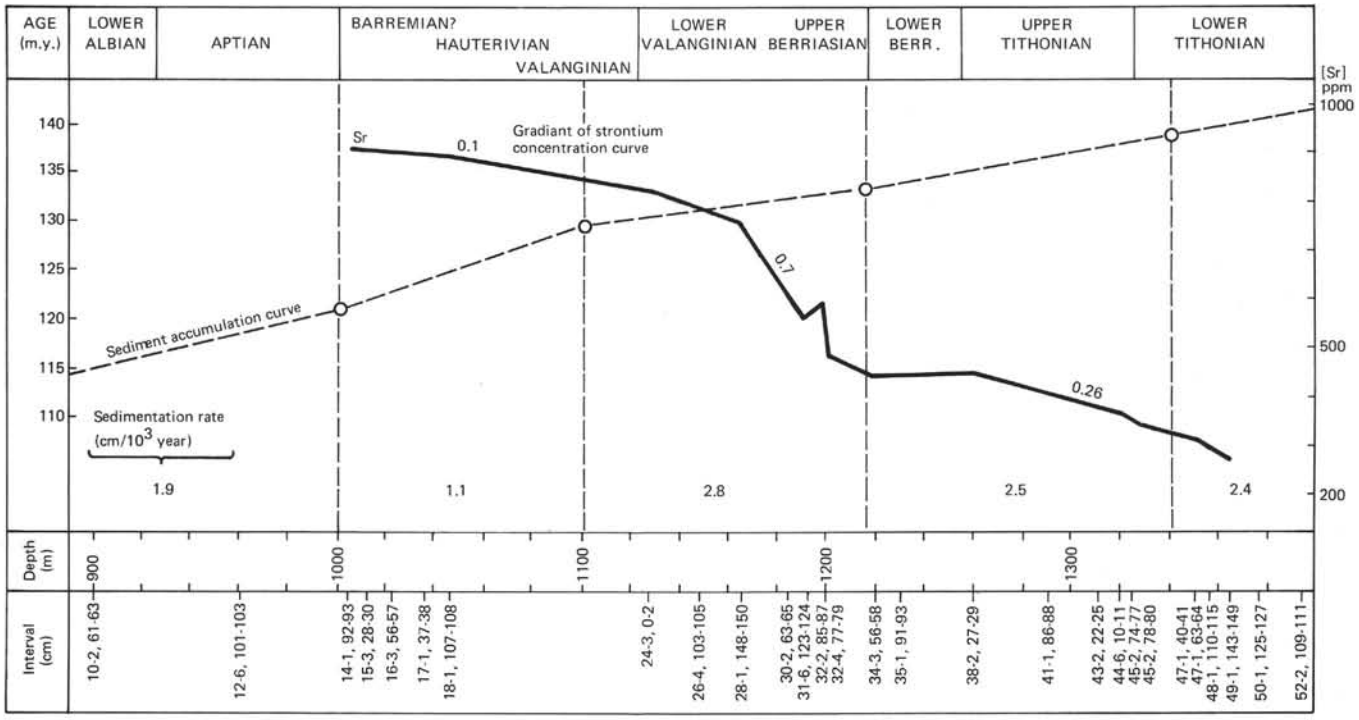

Figure 2. *Distribution of strontium contents in Hole 391C compared with sediment accumulation.*

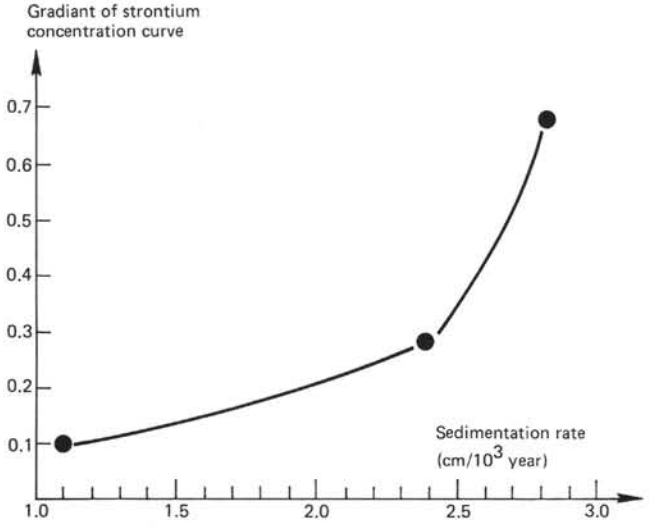

Figure 3. *Correlation between the sedimentation rate and the gradient of the strontium-concentration curve.*

shales. The Fe-Mn diagram (Figure 6) shows the existence of two zones corresponding to different types of sediment supply: those of volcanic origin, characterized by a high Mn/Fe ratio and comprising in particular Tithonian samples; and those of continental origin, characterized by a low Mn/Fe ratio and comprising Valanginian to Barremian samples.

Volcanic materials may have been supplied again during the Albian, but we cannot corroborate this on the basis of available samples. Data for Hole 391C are presented on Table 1.

HOLES 390 AND 390A

Preliminary data for strontium, manganese, and iron from the carbonate fraction are presented in Tables 2 and 3. We did not detect any relationship between the concentrations of these elements and the percentage of insoluble residues.

Strontium

The strontium concentration curve for the Cretaceous part of this interval is similar to that of Hole 391C: strontium continuously decreases from Maestrichtian to Barremian sediments as a function of greater diagenesis with increased age, and a possible contribution from vadose solution (Létolle et al., this volume). The top of zone of decreasing strontium, however, is in Maestrichtian sediments (110 m depth) and hence at a shallower level than in Hole 391C (Valanginian, 1100 m depth).

Near the Cretaceous/Tertiary boundary, the strontium-concentration curve shows a very important discontinuity (Figure 7). A rapid decrease registered in the upper Maestrichtian continues in Danian sediments. In overlying sediments the strontium curve, though generally regular, shows several oscillations from 500 to 750 ppm. For example, the upper boundary of the lower Eocene is characterized by another rapid decrease of the strontium concentration.

Presently we can offer no explanation for these variations although several possibilities exist.

1) Variation of temperature ($K_{Sr\ calcite}$= 0.14 at 25°C = 0.08 at 100°C),
2) Variation of the strontium metabolism of nannofossils,
3) Variation of the ratio Sr^{2+}/Ca^{2+} of seawater,
4) Variation of the clastic carbonate supply.

TABLE 1
Results of Trace Element Analyses, Hole 391C

Sample (Interval in cm)	Sr (ppm)	Mg (ppm)	Na (ppm)	K (ppm)	Mn (ppm)	Zn (ppm)	Fe (ppm)	$CaCo_3$ (%)	Chronostrati.	Lithology
10-2, 61-63	369	3926	3049	462	9469	26	1074	71.45	Lower Albian	Limestone
12-6, 101-103	899	9534	6356	931	241	37	2290	61.46	Aptian	Nannofossil limestone
14-1, 92-93	911	2956	2034	349	290	11	1774	89.19	Barremian ?	Limestone
15-3, 28-30	1163	8131	1784	440	192	10	2965	82.58	Hauterivian	Clayey limestone
16-3, 56-57	2370	13156	11100	2448	383	39	4090	42.80	Lower Valanginian	Limestone with shale
17-1, 97-98	1104	3070	1747	348	513	13	2597	87.49		Sandy limestone
18-1, 107-108	878	6388	5135	1376	614	43	5252	40.09		Sandy limestone
24-3, 0-2	820	2460	1288	193	433	10	890	94.38		Laminated and bioturbated limestone
26-4, 103-105	791	2911	1560	257	483	33	1966	92.63		Laminated and bioturbated limestone
28-1, 148-150	755	2975	1091	160	314	10	2215	99.47		Laminated and bioturbated limestone
30-2, 63-65	610	1886	1220	141	355	11	2074	99.38		Laminated and bioturbated limestone
31-6, 123-124	564	1808	1458	186	241	17	1918	97.75	Upper Berriasian	Laminated and bioturbated limestone
32-2, 85-87	598	1826	1770	188	299	13	2080	95.54		Laminated and bioturbated limestone
32-4, 77-79	489	1724	1245	163	361	12	2168	98.84		Laminated and bioturbated limestone
34-3, 56-58	440	1760	2827	220	1430	16	2282	93.40	Lower Berriasian	Clayey limestone
35-1, 91-93	514	1970	2451	449	1685	13	2254	83.85		Clayey limestone
38-2, 27-29	449	1588	1731	204	789	13	1534	95.47		Limestone
41-1, 86-88	405	2462	1532	167	678	20	1456	97.59		with clayey
43-2, 22-25	373	2559	1356	146	612	30	1502	96.58	Upper Tithonian	stringers
44-6, 10-12	364	2811	1323	142	535	49	1257	96.32		Limestone
45-2, 74-77	343	2659	1307	173	687	54	1196	94.16		Interbedded "green and red"
45-2, 78-80	385	2862	2004	424	738	26	991	79.44		limestone
47-1, 40-41	611	3931	5460	1048	1463	28	437	60.63		Clayey limestone
47-1, 63-67	314	2975	1168	207	2700	21	1080	90.16	Lower	Limestone
48-1, 110-113	906	5355	519	1005	2010	37	746	62.83	Tithonian	Limestone with clay stringers
49-1, 143-149	299	2825	124	148	3531	33	904	97.34		Limestone
50-1, 125-127	1239	5994	10656	1572	2131	46	333	52.03		Calcareous claystone
52-2, 109-111	3862	7347	15084	1742	9103	64	733	40.93		Claystone (volc. glass)

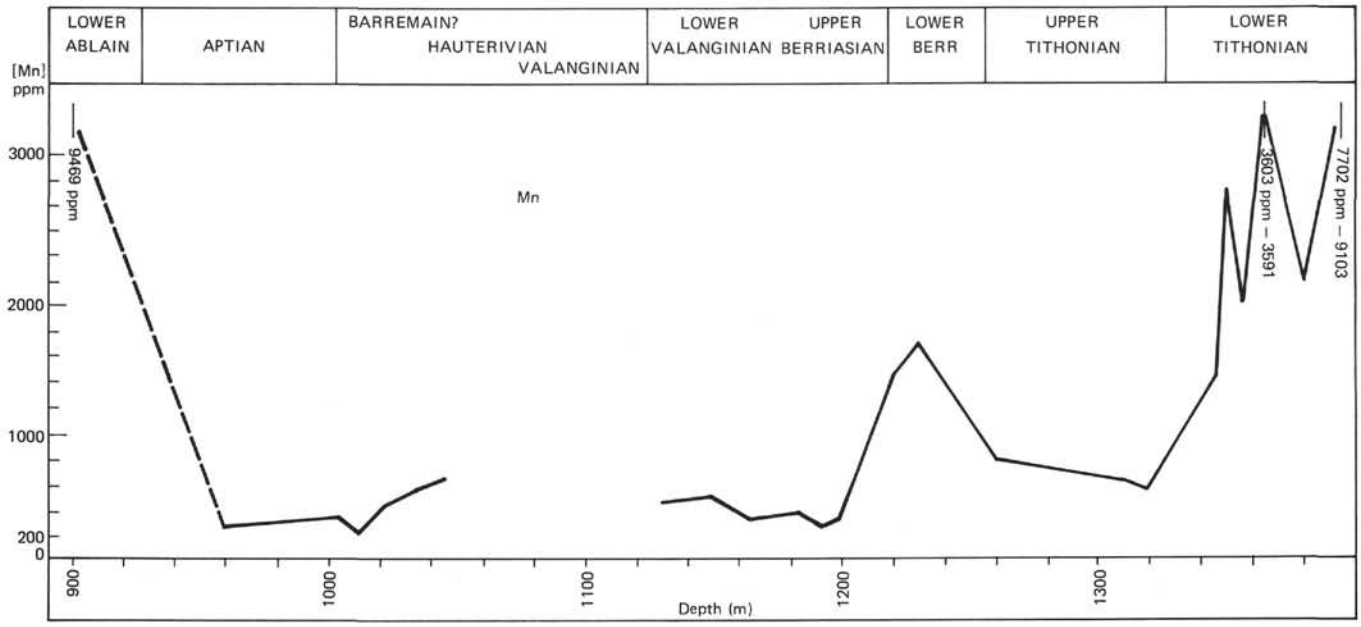

Figure 4. *Distribution of manganese contents in Hole 391C.*

TABLE 2
Results of Trace Element Analyses, Hole 390

Sample (Interval in cm)	Sr (ppm)	Mn (ppm)	Fe (ppm)	$CaCO_3$ (%)	Chronostrat.	Lithology
1-1, 135-136	521	194	25	96.49	Middle Eocene	Nannofossil ooze
1-3, 86-87	570	204	21	93		Nannofossil ooze
1-6, 85-86	620	237	27	96.25		Nannofossil ooze
3-1, 112-114	672	103	244	49.29	Campanian	Nannofossil clay
3-3, 129-131	548	72	396	34.95		Nannofossil clay
3-3, 147-149	498	239	355	38.07		Nannofossil clay
5-1, 133-134	236	186	62	59.24	Lower Albian-Barremian	Nannofossil chalk
5-2, 138-140	293	167	431	72.54		Nannofossil chalk (with mudstone)
6-1, 126-128	152	268	177	99.79		Calcareous ooze homogenized by drilling
8-2, 51-53	234	176	118	95.52	Barremian ?	Calcareous sand and gravel
8-4, 131-133	164	17	48	91.01		Chalk clasts and calcareous mudstone
8-6, 143-144	145	16	37	91.51		Calcareous mud
9-1, 78-80	119	12	60	98.42		Calcareous pseudogravel and mudstone

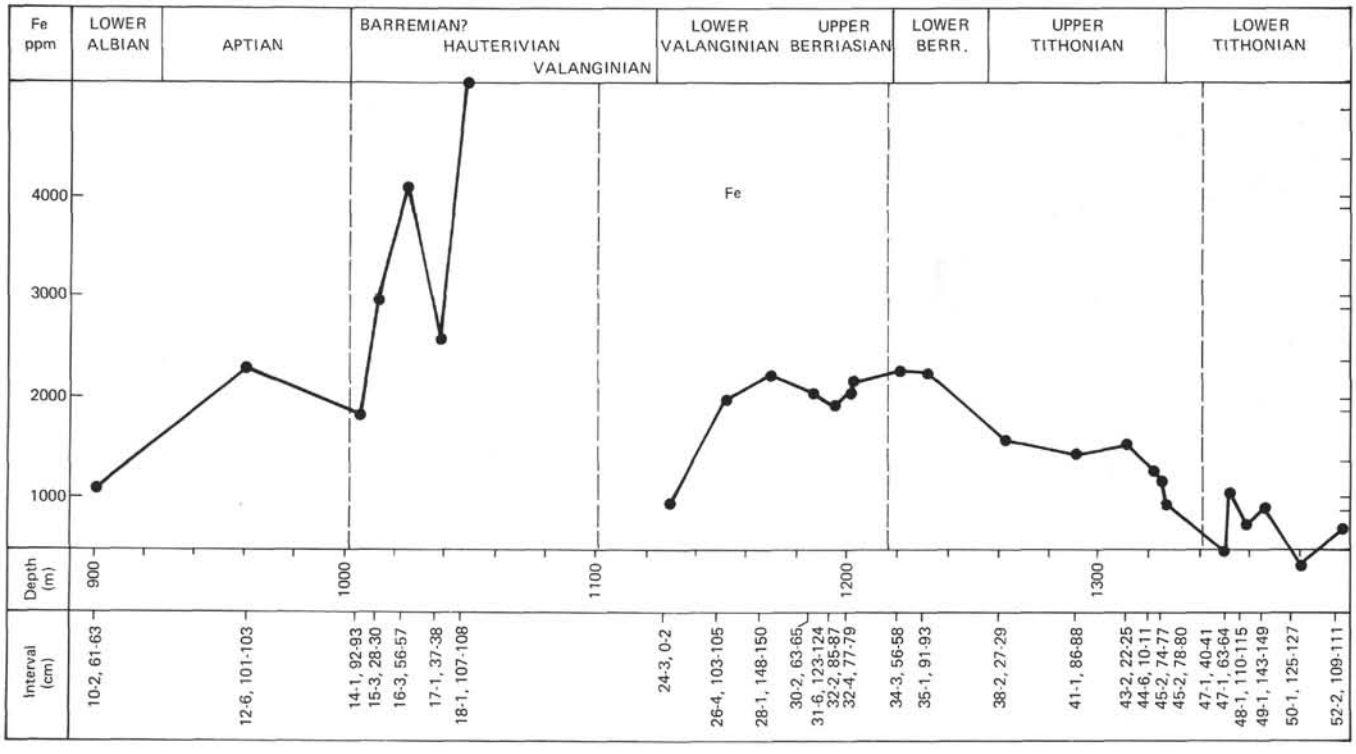

Figure 5. *Distribution of iron contents in Hole 391C.*

We can speculate that the Tertiary oscillations reflect the beginning of a connection between the Atlantic and Arctic oceans, but we cannot presently present conclusive evidence in support of that view. The range and average strontium concentrations at different stratigraphic levels are given in Figure 8.

Manganese

The manganese concentrations at Holes 390 and 390A are always lower than 500 ppm (Figure 9). The amounts measured for Barremian samples are similar to those for corresponding samples in Hole 391C. The Albian samples, however, never have high manganese concentrations. Manganese concentrations decrease above the Tertiary/Cretaceous boundary although the decrease is less distinct than that of strontium. The lower Eocene sediments are poor in manganese and the upper boundary of the middle Miocene is marked by a rapid increase in manganese. These variations are not related to volcanic activity but to oxidation-reduction mechanisms; thus three sequences must have been deposited under reducing conditions.

1) The lower Eocene (Samples 5-1, 70-72 to 7-4, 138-140 cm);
2) The lower Maestrichtian (Samples 390A-14-1, 12-14 cm to 14-5, 5-7 cm; Hole 390A);
3) Part of the Barremian (Samples 390-8-4, 131-133 cm to 9-1, 78-80 cm).

TABLE 3
Results of Trace Element Analyses, Hole 390A

Sample (Interval in cm)	Sr (ppm)	Mn (ppm)	Fe (ppm)	$CaCo_3$ (%)	Chronostrat.	Lithology
1-1, 94-96	544	349	28	89.72		Nannofossil ooze
2-2, 46-48	521	422	22	78.07		Nannofossil ooze
3-2, 72-73	628	222	34	79.24	Middle Eocene	Siliceous nannofossil ooze
3-4, 109-110	694	208	29	83.33		Siliceous nannofossil ooze
4-1, 95-96	514	441	10	81.12		Siliceous nannofossil ooze
4-5, 86-87	515	451	22	79.86		Siliceous nannofossil ooze
4-6, 106-107	578	302	28	72.87		Nannofossil chalk
5-1, 70-72	765	59	34	89.04		Nannofossil ooze
5-2, 135-136	749	74	14	82.50		Nannofossil chalk
6-1, 26-28	742	87	23	86.03		Nannofossil ooze
6-3, 90-91	738	80	17	72.18		Siliceous nannofossil ooze
6-5, 89-91	698	68	20	76.27	Lower Eocene	Nannofossil ooze
6-6, 89-90	660	64	20	88.07		Siliceous nannofossil ooze
7-1, 131-133	555	65	132	64.02		Nannofossil ooze
7-2, 79-80	518	79	48	67.80		Siliceous nannofossil ooze
7-4, 138-140	544	71	33	54.62		Siliceous nannofossil ooze
8-2, 54-56	815	172	156	35.94		Nannofossil chalk
8-4, 126-128	625	271	42	61.14		Nannofossil ooze
9-1, 120-122	523	82	33	60.24	Lower Paleocene	Zoolitic nannofossil ooze
10-1, 84-86	564	151	99	76.46		Marly nannofossil ooze
10-3, 80-82	726	229	43	62.15		Marly nannofossil ooze
10-6, 90-92	883	295	35	63.40		Marly nannofossil ooze
11-1, 134-136	725	256	32	68.18		Nannofossil ooze
11-2, 128-129	803	285	41	75.60		Nannofossil ooze
11-4, 100-102	828	284	39	78.45		Marly nannofossil ooze
11-6, 121-123	1062	466	153	85.10		Marly nannofossil ooze
12-1, 48-50	1145	420	146	80.28		Nannofossil ooze
12-3, 70-72	1128	433	152	74.28		Nannofossil ooze
12-6, 31-39	996	432	253	84.61		Nannofossil ooze
13-1, 117-119	999	442	179	81.92	Maestrichtian	Nannofossil ooze
13-3, 84-86	849	320	93	91.22		Nannofossil ooze
13-6, 89-91	808	283	71	98		Nannofossil ooze
14-1, 12-14	798	93	36	98.10		Nannofossil ooze
14-3, 80-82	928	99	62	89.67	?	Nannofossil ooze
14-5, 5-7	808	93	35	99.58	Upper Campanian	Marly nannofossil ooze

TABLE 4
Results of Trace Element Analyses, Hole 392A

Sample (Interval in cm)	Sr (ppm)	Mn (ppm)	Fe (ppm)	$CaCO_3$ (%)	Chronostrat.	Lithology
1-1, 124-126	715	39	23	90.39	Upper Campanian	Foram-nannofossil ooze
1-2, 144-145	956	83	46	89.39	Upper Campanian	Foram-nannofossil ooze
2-1, 49-50	1630	130	953	53.17	Lower Albian	Marly-nannofossil ooze
2-2, 19-23	308	175	377	72.20	Lower Albian	Marly-nannofossil ooze
3-1, 102-104	737	144	667	53.13	Upper Aptian	Marly-nannofossil ooze
3-2, 105-106	259	139	135	86.31	Upper Aptian	Nannofossil ooze
3-3, 70-71	232	89	57	69.51	Upper Aptian	Nannofossil ooze
4-1, 125-126	952	122	391	44.40	Barremian	Lime mudstone

Iron

The iron-concentration curve for Holes 390 and 390A is very different for the Cretaceous and Tertiary sediments (Figure 10). The latter, notably the Eocene, is homogeneous and poor in iron ($\times 100$ ppm), whereas the iron concentrations in Cretaceous sediments are generally higher and more variable. In contrast to strontium and manganese, iron concentrations are not noticeably different toward the top of the lower Eocene.

HOLE 392A

We do not have enough samples from this hole to adequately describe a general geochemical evolution, but the concentration curves of strontium, manganese, and iron seem to show the same trend as seen in sediments from Hole 390A (Figure 11). The rapid decrease of strontium concentrations down section through the Albian sediments is particularly evident. The values of the manganese concentrations are the same in Holes 390A and 392A. As in Hole

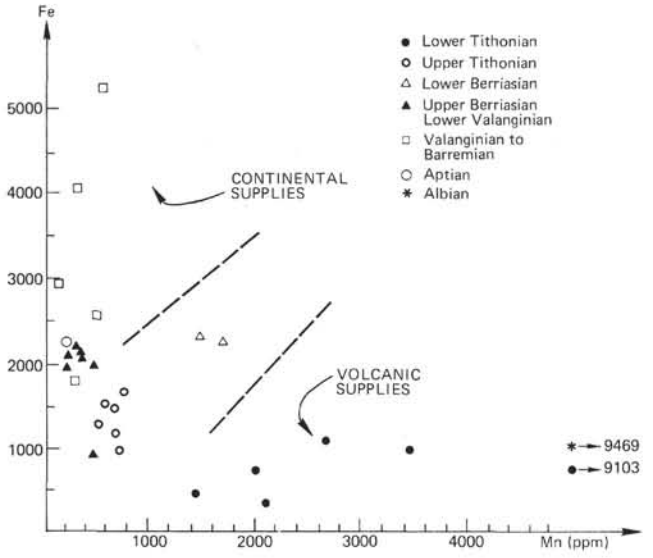

Figure 6. *Relationship between manganese and iron concentrations in Hole 391C.*

390A the iron curve shows a great variability, but in Hole 392A the iron concentrations are higher.

ACKNOWLEDGMENTS

This work was performed with the assistance of the Centre National d'Exploitation des Océans (France).

We are grateful to Mr. Michel Petzold for preparation of the figures and to Mrs. Chantal Odin for typing various drafts of the manuscript. We thank also Mr. Olivier Canaveso, and Mr. and Mrs. Kleyn for correction of the English text.

REFERENCES

Kinsmann, D.J.J., 1969. Interpretation of Sr^{2+} concentrations in carbonate minerals and rocks: *J. Sediment. Petrol.*, 39, p. 486-508.

Michard, G., 1969. Contribution a l'étude du comportement du Manganèse dans sédimentation: *Thèse,* Univ. Paris.

_____, 1975. L'action de l'eau de mer sur les basaltes, source possible du manganèse. Etude thermodynamique préliminaire: *C.R. Acad. Sci Paris,* v. 280, ser. D, p. 1213-1215.

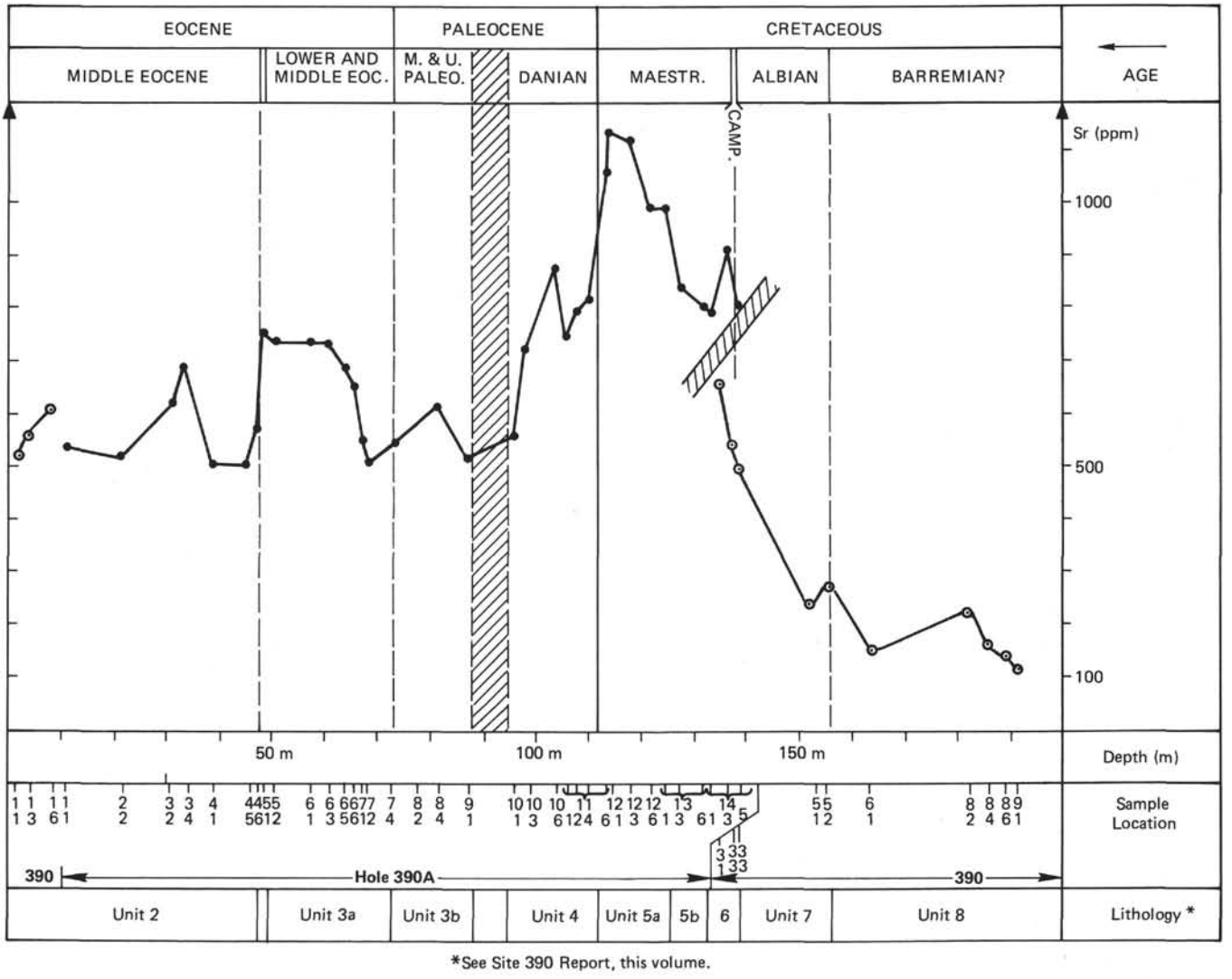

*See Site 390 Report, this volume.

Figure 7. *Strontium concentrations in Holes 390, 390A.*

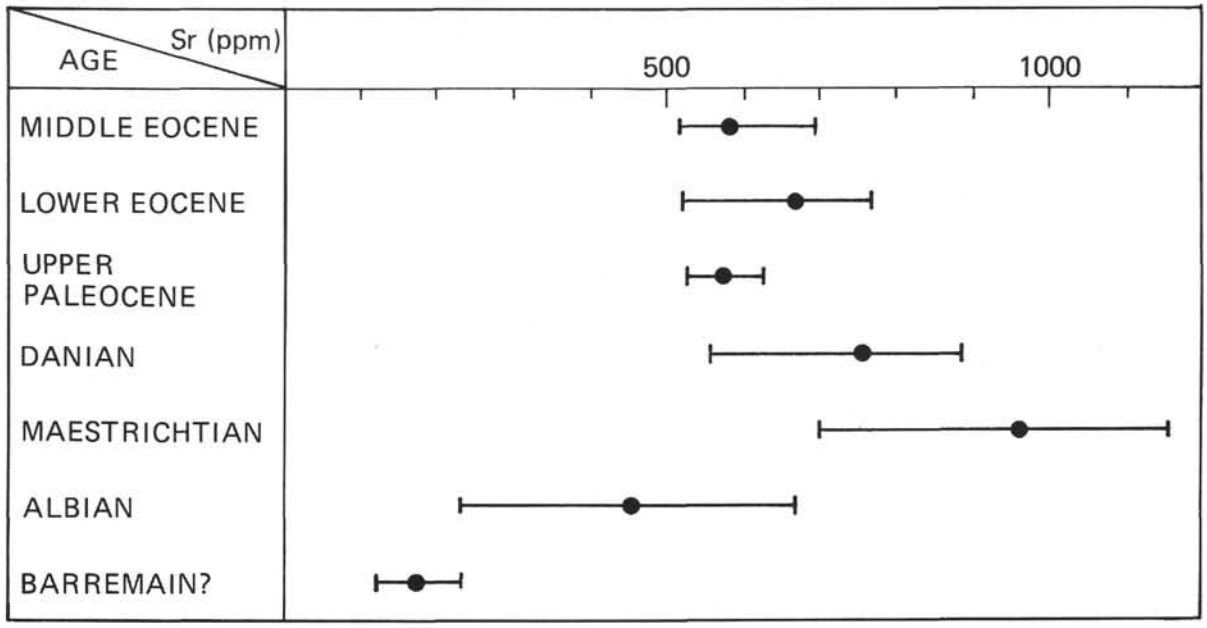

Figure 8. *Range and average strontium concentrations in the different stratigraphic levels in Holes 390, 390A.*

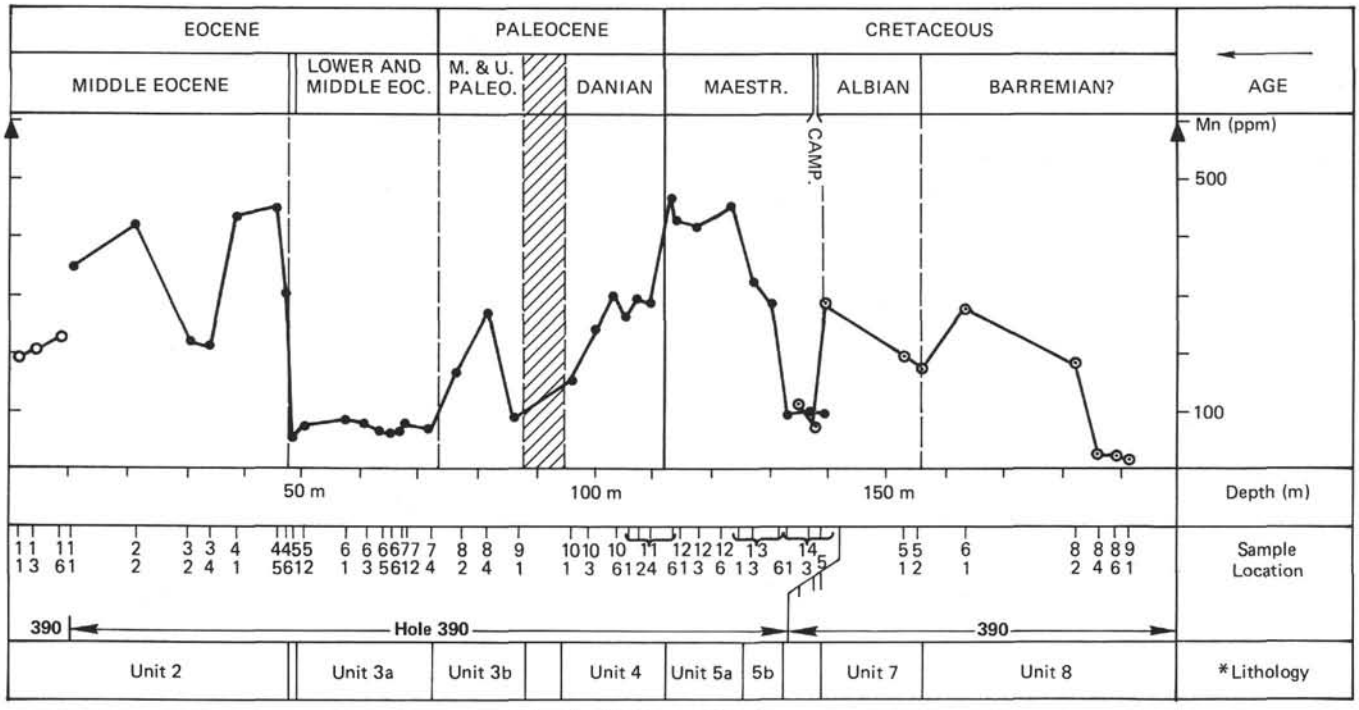

*See Site 390 Report, this volume.

Figure 9. *Manganese concentrations in Holes 390, 390A.*

Renard, M. and Blanc Ph., 1971. Mise au point d'un protocole ex perimental pour le dosage d'éléments en traces (V, Cr, Mn, Ni, Sr, Mo) par absorption atomique: *C.R. Acad. Sci. Paris, clv. 272, p. 2285-2288.*

———, *1972. Influence des conditions de mise en solution (choix de l'acide, tem*pérature et durée d'attaque) dans le dosage des eleḿents en traces des roches carbonatées: *C.R. Acad. Sci. Paris,* v. 274, p. 632-635.

Renard, M., 1972. Interpretation des teneurs en strontium des carbonates du Lutétien supérieur a St Vaast-les-Mello (Oise). Mise en évidence de la valeur de cet élément comme indicateur des conditions de diagenèse et de sédimentation des carbonates: *Bull. Assoc. Géol. Bassin Paris,* v. 34, p. 19-29.

Sherman, D.J. and Shirmohammadi, N.H., 1969. Distribution of strontium in dolomites from the French Jura: *Nature,* v. 208, p. 1310-1311.

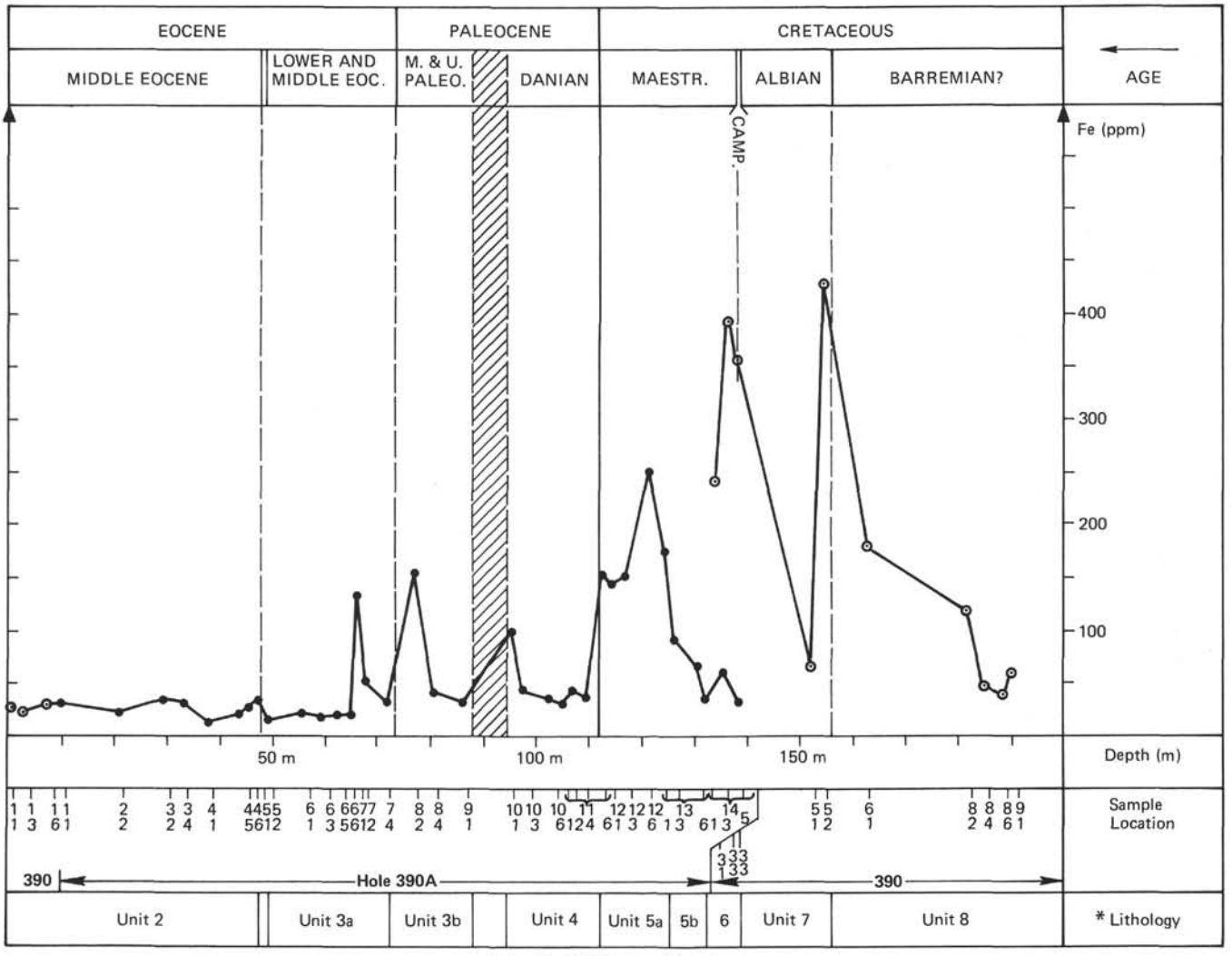

* See Site 390 Report, this volume.

Figure 10. *Iron concentrations in Holes 390, 390A.*

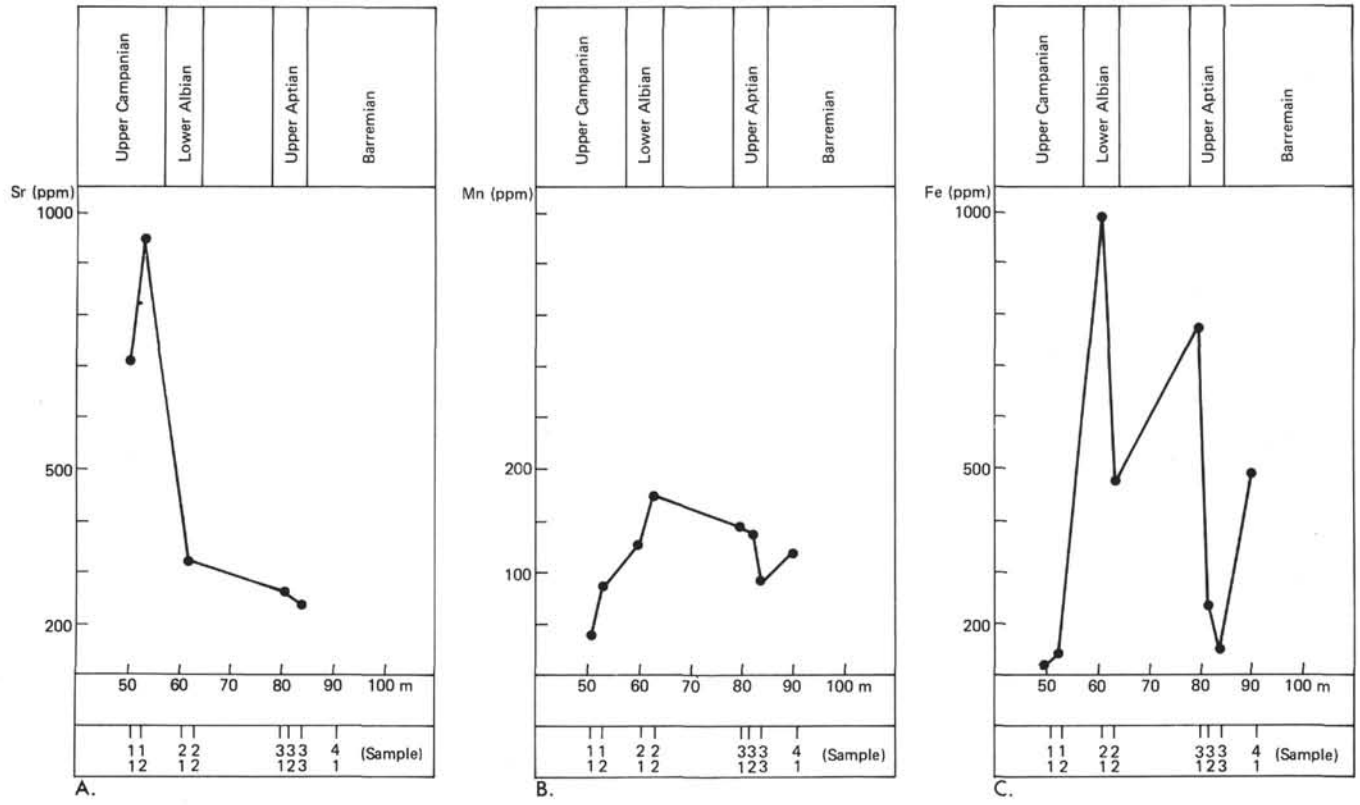

Figure 11. *Concentrations of strontium (A), manganese (B), and iron (C) at Hole 392A.*